

Displacement-noise-free gravitational-wave detection with a single Fabry-Perot cavity: a toy model

Sergey P. Tarabrin and Sergey P. Vyatchanin

*Faculty of Physics, Moscow State University, Moscow, 119992, Russia**

(Dated: April 24, 2008)

We propose a detuned Fabry-Perot cavity, pumped through both the mirrors, as a *toy model* of the gravitational-wave (GW) detector partially free from displacement noise of the test masses. It is demonstrated that the noise of cavity mirrors can be eliminated, but the one of lasers and detectors cannot. The isolation of the GW signal from displacement noise of the mirrors is achieved in a proper linear combination of the cavity output signals. The construction of such a linear combination is possible due to the difference between the reflected and transmitted output signals of detuned cavity. We demonstrate that in low-frequency region the obtained displacement-noise-free response signal is much stronger than the f_{gw}^3 -limited sensitivity of displacement-noise-free interferometers recently proposed by S. Kawamura and Y. Chen. However, the loss of the resonant gain in the noise cancelation procedure results in the sensitivity limitation of our toy model by displacement noise of lasers and detectors.

PACS numbers: 04.30.Nk, 04.80.Nn, 07.60.Ly, 95.55.Ym

I. INTRODUCTION

Currently the search for gravitational radiation from astrophysical sources is conducted with the first-generation Earth-based laser interferometers [1, 2] (LIGO in USA [3, 4, 5], VIRGO in Italy [6, 7], GEO-600 in Germany [8, 9], TAMA-300 in Japan [10, 11] and ACIGA in Australia [12, 13]). The development of the second-generation GW detectors (Advanced LIGO in USA [14, 15], LCGT in Japan [16]) is underway.

The sensitivity of the first-generation detectors is limited by a great amount of noises of various nature: seismic and gravity-gradient noise at low frequencies (below ~ 50 Hz), thermal noise in suspensions, bulks and coatings of the mirrors ($\sim 50 \div 500$ Hz), photon shot noise (above ~ 500 Hz), etc. It is expected that the sensitivity of the second-generation detectors will be limited by the noise of quantum nature arising due to Heisenberg's uncertainty principle: the more precise is the measurement of the test mass coordinate, the more disturbed becomes its momentum which in turn evolves into the disturbance of the coordinate, thus ultimately limiting the sensitivity [17]. The optimum between measurement noise (photon shot noise) and back-action noise (radiation pressure noise) is called the Standard Quantum Limit (SQL) [18, 19, 20].

Though the start of operation of the second-generation detectors is planned for the next decade, the theoretical investigations of the third-generation prototypes have already begun [21, 22, 23, 24, 25, 26]. It is expected that the barrier of SQL will be overcome and the sensitivity of the third-stage detectors will be at least an order of magnitude better than the SQL of a free mass.

Recently in a series of papers [27, 28, 29] S. Kawamura and Y. Chen proposed several topologies of the

GW detectors, both ground- and space-based, which are free from displacement noise of the test masses. It was pointed out there that in order the GW detector to be a truly displacement-noise-free interferometer (DFI) it should be also free from optical laser noise which is indistinguishable from laser displacement noise. Cancellation of the optical noise in interferometric experiments is usually achieved by implementing the differential schemes of measurements: in conventional interferometers (such as LIGO) it is the Michelson topology and in DFIs proposed in Ref. [29] it is the Mach-Zehnder (MZ) topology.

The most intriguing feature of displacement-noise-free interferometry is the straightforward overcoming of the SQL (since radiation pressure noise is canceled) without the need of implementation of very complicated and vulnerable schemes for Quantum-Non-Demolition (QND) measurements [21, 30, 31, 32]. One only needs to increase the laser power to suppress quantum shot noise and achieve the arbitrarily high sensitivity.

The isolation of the GW signal from fluctuating displacements of the test masses in the DFI schemes proposed by S. Kawamura *et al.* is possible due to the fact that the interaction of GWs with a laser interferometer is distributed, as viewed from both the transverse-traceless (TT) gauge [33, 34, 35] and the local Lorentz (LL) gauge [35, 36, 37].

In the TT gauge test masses are immovable, i.e. have fixed spacial coordinates and thus do not sense the gravitational wave. However, GW couples to the light wave in this gauge producing a non-vanishing phase shift. This can be thought of as an apparent change of the coordinate velocity of light. Even if the test masses are not ideally inertial and follow non-geodesic motion then the interferometer will respond differently to the test masses motions and the gravitational wave. This difference allows the cancelation of displacement noise in a proper linear combination of the interferometer response signals.

From the viewpoint of local observer (the LL gauge)

*Electronic address: tarabrin@phys.msu.ru

the interaction of GW with a laser interferometer adds up to two effects. The first one is the motion of the test masses in the GW tidal force-field. In this aspect GWs are indistinguishable from any non-GW forces since both are sensed by the light wave only in the moments of reflection from the test masses. If the linear scale L of a GW detector is much smaller than the gravitational wavelength λ_{gw} (the so-called long-wave approximation) then the effect of the GW force-field is of the order of $h(L/\lambda_{\text{gw}})^0$, where h is the absolute value of the GW amplitude. The relative motion of the test masses, separated by a distance L , in any force field cannot be sensed by one of them faster than L/c , thus resulting in the rise of terms of the order of $O[h(L/\lambda_{\text{gw}})^1]$ describing time delays. Second, GW directly couples to the light wave effectively changing the coordinate velocity of light (but in a different manner as compared to the TT gauge). In long-wave approximation this effect has the order of $O[h(L/\lambda_{\text{gw}})^2]$. Therefore, in terms of the LL gauge displacement-noise-free interferometry necessarily implies the cancelation of the information about non-GW forces along with the GW force-field leaving a non-vanishing information about the direct coupling of the GW to light.

The analysis performed by S. Kawamura *et al.* in Ref. [29] showed, however, that though it is possible to eliminate all the information about displacement and laser noises from the data, the sensitivity to GWs at low frequencies turns out to be limited by the $(\omega_{\text{gw}}L/c)^2$ -factor for 3D (space-based) configurations and $(\omega_{\text{gw}}L/c)^3$ -factor for 2D (ground-based) configurations. In the latter case this means the cancelation of all the terms of the order of $h(L/\lambda_{\text{gw}})^n$, $n = 0, 1, 2$. For the signals around $\omega_{\text{gw}}/2\pi \approx 100$ Hz and $L \approx 4$ km, the DFI sensitivity of the ground-based detector is $\sim 10^6$ times worse than the one of the conventional Michelson interferometer (i.e. a single round-trip detector). The proposed MZ-based configurations could be modified with power- and signal-recycling mirrors, artificial time-delay devices [38], but nevertheless, the potentially achievable sensitivity remains incomparable with conventional non-DFI detectors.

In this paper we continue investigation of the noise cancelation issue in large-scale interferometric experiments and propose a simple toy model of the GW detector *partially* free from displacement noise of the test masses with strong enough GW response. The basic element of our model is a single detuned Fabry-Perot (FP) cavity pumped through both of its movable, partially transparent mirrors; lasers and detectors are assumed to be located on auxiliary (also movable) platforms. Pump waves in different input ports are assumed to be orthogonally polarized in order the corresponding output waves to be separately detectable and to exclude nonlinear coupling of the corresponding intracavity waves. By properly combining the signals of all four output ports of the cavity (a pair of reflection and transmission ports for each of the pumps) an experimentalist can remove the information about the fluctuations of the mirrors coordinates from

the data. Below we call the proposed scheme a double-pumped Fabry-Perot (DPFP) cavity. In this paper we do not consider the problem of optical laser noise cancelation and thus “displacement noise” refers only to the mechanical motions of the test masses further. We will consider a FP cavity with the mirrors having equal transmittances. The case of different transmittances will be analyzed separately [39].

The isolation of the GW signal from displacement noise in a DPFP cavity is achieved in a different manner as compared to MZ-based interferometers. The basic idea is that when a detuned FP cavity is pumped through one of the mirrors (mirror a for definiteness), the reflected and transmitted waves respond differently to the motion of mirrors a and b . The physical reason for this is that the reflected wave, in contrast to the transmitted one, includes the component due to the prompt reflection from mirror a . This component measures only the position of mirror a but not the position of mirror b . By properly combining both the response signals one can eliminate the information about the fluctuating coordinate of mirror a completely, leaving only the part of the signal containing the displacement noise of mirror b plus its displacement due to GW (assuming we work in the local Lorentz frame of mirror a). By pumping the cavity through mirror b and performing the similar operations, one can eliminate the information about displacement noise of mirror b . Ultimately, the proper linear combination of all four output signals cancels displacement noise of both the mirrors leaving a non-vanishing GW signal.

In the resonant regime both the response signals (corresponding to one of the pumps) carry identical information about the mirrors coordinates and thus cannot be combined to cancel their fluctuations. This happens because the prompt reflection does not occur for the resonant pump.

Note that the LL-effect of GW direct coupling to light plays no role in this noise-cancelation scheme: the notion of the GW in our analysis can be approximated with the corresponding tidal force-field. This means that the leading order of the DFI signal we obtain will be $h(L/\lambda_{\text{gw}})^0$.

The “payment” for isolation of the GW signal from displacement noise in our case is the loss of the optical resonant gain of the order of $c/(\gamma L)$, where γ is the cavity half-bandwidth. In conventional interferometers this resonant factor describes the accumulation of the low-frequency GW signal by the light wave circulating in a FP cavity. The DFI response signal of a DPFP cavity becomes limited with the factor of the order of unity as compared to the limiting factor $(\omega_{\text{gw}}L/c)^3 \sim 6 \times 10^{-7}$ of the double Mach-Zehnder configuration [29] for $L \approx 4$ km and $\omega_{\text{gw}}/2\pi \approx 100$ Hz. This difference between the MZ-based topologies and the DPFP topology arises due to the different mechanisms of noise cancelation: the former utilizes the LL-effect of direct interaction between the GW and light while the latter utilizes the asymmetry between the output signals of detuned cavity.

However, the most dramatic consequence which the

loss of the resonant gain results in is that the displacement noise of the auxiliary platforms (where lasers and detectors are mounted) becomes comparable to the DFI response. The reason for this is the relativity principle itself: only relative measurements of the test masses positions and velocities are allowed; in our case we are able to measure the positions of cavity mirrors only with respect to the mentioned auxiliary platforms. It is natural then that the precision of the coordinate measurements is limited with the noises of reference test masses (see discussion in Sec. V further). Remind also that in conventional non-DFI (LIGO) topology these noises are negligible since they are suppressed finesse times as compared to the GW signal (and displacement noise of the mirrors). The incomplete cancelation of displacement noise is the major drawback of our toy model. To increase its SNR in practice one will need to install lasers and detectors on heavy platforms (to suppress displacement noise due to external forces) cooled down to cryogenic temperatures (to suppress internal thermal noise).

Note that the non-resonant regime implies the rise of the electromagnetic ponderomotive force (and corresponding optical rigidity) acting on the mirrors of a FP cavity [40, 41, 42, 43, 44, 45, 46, 47, 48]. However, in this paper we do not take into account the effects of radiation pressure. In particular, optical rigidity vanishes if pump waves in different input ports have detunings with equal absolute values but opposite signs.

This paper is organized as follows. In Sec. II we introduce the space-time associated with the accelerated observer in the field of weak GW. In Sec. III we derive the response signals of a Fabry-Perot cavity, pumped through one of the mirrors, to a gravitational wave of arbitrary frequency using the method developed in Refs. [37] and [49]. In Sec. IV we consider the responses of a double-pumped Fabry-Perot cavity and introduce their proper linear combination which cancels the fluctuating displacements of the mirrors. Finally in Sec. V we discuss the physical meaning of the obtained results and briefly outline the further prospects associated with laser noise cancelation.

II. SPACE-TIME OF ACCELERATED OBSERVER IN THE GRAVITATIONAL WAVE FIELD

A. Motion of the test masses

In the Earth-bound GW observatories all the test masses including lasers and detectors undergo fluctuative motions. Since it is the detector that produces an experimentally observable quantity one should consider the operation of an interferometer in its proper reference frame, which is non-inertial in general. For this purpose we first introduce the space-time associated with an observer having non-geodesic 3-acceleration $\ddot{\xi}_i(t) = \{\ddot{\xi}_x(t), \ddot{\xi}_y(t), \ddot{\xi}_z(t)\}$ and falling in the GW field

$h = h(t - z/c)$. We assume the latter to be weak, plane, '+'-polarized and propagating along the z -axis. The case of generic GW polarization and direction of propagation does not introduce any significant changes (in the context of this work) to our further analysis. Therefore, in the proper reference frame of such an observer space-time metric takes the following form [35, 36, 37, 49, 50, 51, 52]:

$$ds^2 = - (cdt)^2 \left[1 + \frac{2}{c^2} \ddot{\xi}_i(t) x^i \right] + dx^2 + dy^2 + dz^2 + \frac{1}{2} \frac{x^2 - y^2}{c^2} \ddot{h}(t - z/c) (cdt - dz)^2. \quad (1)$$

Latin indices run over 1, 2, 3. In this paper we consider only one-dimensional motion of the test masses, thus without the loss of generality we may assume $y = z = 0$ and denote $\xi_x(t) \equiv \xi(t)$. In practice fluctuative forces acting on the test masses are very weak, as the GW itself, thus it is natural to require that for all reasonable x and t conditions $|2\ddot{\xi}x/c^2| \ll 1$ and $|h| \ll 1$ are fulfilled so we can use the methods of linearized theory.

Metric (1) has two special cases.

1. $\ddot{\xi}(t) = 0$ and the proper reference frame coincides with the local Lorentz frame (also called the LL gauge in literature) of the observer freely falling in the GW field. It is worth noting that the LL gauge is free from the requirement of the distance L between the test masses to be much smaller than the gravitational wavelength λ_{gw} [36, 37]. Corresponding approximation $L \ll \lambda_{\text{gw}}$ will be called below the long-wave approximation.
2. $h(t) = 0$ and the proper reference frame is simply a non-inertial frame in Newtonian sense. Note that the curvature of space-time with metric (1) equals to zero under this condition, since it can be made globally flat with the coordinate transformation that brings us from the non-inertial frame to the inertial one.

Remind, that due to the relativity principle an observer is unable to measure his non-geodesic displacement $\xi(t)$ absolutely, in contrast to the corresponding acceleration $\ddot{\xi}(t)$. To avoid the ambiguity associated with the choice of initial conditions $\xi(0)$ and $\dot{\xi}(0)$ we assume below that $\xi(t)$ is measured in such a globally inertial (laboratory) reference frame in the absence of the GW, that $\ddot{\xi}(t) = 0$ results in $\xi(t) = 0$.

The solution to geodesic equation corresponding to metric (1) can be found in Ref. [49]. If the j th test mass and an observer are separated by a distance L on the average (the 0th order solution) then the test mass displacement relative to an observer (the 1st order solution) equals to $X_j(t) = \frac{1}{2}Lh(t) - \xi(t)$. If, in addition, the test mass is subjected to some non-GW forces and undergoes corresponding fluctuative displacement $\xi_j(t)$ (measured in the globally inertial reference frame) then

$$X_j(t) = \frac{1}{2}Lh(t) + \xi_j(t) - \xi(t). \quad (2)$$

Below we assume that for any test mass both its displacements $X_j(t)$ and $\xi_j(t)$ obey the relation $|X_j|, |\xi_j| \ll L$. We will also widely use the spectral domain where

$$\begin{bmatrix} X_j(t) \\ \xi_j(t) \end{bmatrix} = \int_{-\infty}^{+\infty} \begin{bmatrix} X_j(\Omega) \\ \xi_j(\Omega) \end{bmatrix} e^{-i\Omega t} \frac{d\Omega}{2\pi}.$$

The introduced proper reference frame is the best suited for analysis of the GW detectors with the test masses undergoing non-geodesic motion, in contrast to the transverse-traceless (TT) gauge, where such an analysis should be additionally validated. In addition, proper reference frame is the natural frame used by Newtonian experimentalists performing measurements in the laboratory and recording the obtained data from detectors.

B. Quantized electromagnetic wave interacting with the weak gravitational wave in a non-inertial frame

In the interferometric experiments an observer studies the motion of the test masses by sending and receiving the reflected light waves. Thus it is necessary to take into account the effects imposed by the GW and acceleration fields on the optical field for a complete description of an interferometer. Here we briefly remind the formalism used to describe the quantized electromagnetic wave (EMW) propagating in the space-time with metric (1).

First, we start from the simplest case of Minkowski space-time. It is convenient to represent the electric field operator of the EMW as a sum of (i) the “strong” (classical) plane monochromatic wave (which approximates the light beam with cross-section S) with amplitude A_0 and frequency ω_0 and (ii) the “weak” wave describing quantum fluctuations of the electromagnetic field (see Appendix A):

$$A(x, t) = \sqrt{\frac{2\pi\hbar\omega_0}{Sc}} \left[A_0 + a(x, t) \right] e^{-i(\omega_0 t \mp k_0 x)} + \text{h.c.},$$

$$a(x, t) = \int_{-\infty}^{+\infty} a(\omega_0 + \Omega) e^{-i\Omega(t \mp x/c)} \frac{d\Omega}{2\pi},$$

with amplitude $a(\omega_0 + \Omega)$ (Heisenberg operator to be strict) obeying the commutation relations:

$$\begin{aligned} [a(\omega_0 + \Omega), a(\omega_0 + \Omega')] &= 0, \\ [a(\omega_0 + \Omega), a^\dagger(\omega_0 + \Omega')] &= 2\pi\delta(\Omega - \Omega'). \end{aligned}$$

This notation for quantum fluctuations $a(x, t)$ will be the most suitable for us since it coincides exactly with the Fourier-representation of the classical fields. For brevity throughout the paper we omit the $\sqrt{2\pi\hbar\omega_0/Sc}$ -multiplier and notation “h.c.” We call $A(x, t)$ the vacuum-state wave if $A_0 = 0$.

Electromagnetic wave propagating in space-time with metric (1) directly couples to the GW and acceleration

fields. We will study only the 1st order (in h and ξ) coupling effects and neglect the GW and acceleration interaction with the optical noise. In other words, both the GW and acceleration fields are assumed to be coupled only to the “strong” (classical) wave [37, 49]:

$$A(x, t) = \left[A_0 + A_0 g_\pm(x, t) + A_0 w_\pm(x, t) + a(x, t) \right] \times e^{-i(\omega_0 t \mp k_0 x)}, \quad (4)$$

where

$$g_\pm(x, t) = \int_{-\infty}^{+\infty} g_\pm(x, \omega_0 + \Omega) e^{-i\Omega t} \frac{d\Omega}{2\pi},$$

$$g_\pm(x, \omega_0 + \Omega) = h(\Omega) \left[\frac{1}{4} \omega_0 \Omega \frac{x^2}{c^2} \mp i \frac{1}{2} k_0 x + \frac{1}{2} \frac{\omega_0}{\Omega} \left(e^{\pm i\Omega x/c} - 1 \right) \right],$$

and

$$w_\pm(x, t) = \int_{-\infty}^{+\infty} w_\pm(x, \omega_0 + \Omega) e^{-i\Omega t} \frac{d\Omega}{2\pi},$$

$$w_\pm(x, \omega_0 + \Omega) = -k_0 \xi(\Omega) \left[\frac{\Omega}{c} x \pm i \left(e^{\pm i\Omega x/c} - 1 \right) \right].$$

Both $g_\pm(x, t)$ and $w_\pm(x, t)$ describe the distributed effects: g_\pm is responsible for the direct coupling between the GW and the EMW and w_\pm describe the redshift imposed on the EMW by the non-inertiality of the reference frame. Both terms are accurate up to the order of $(\Omega/\omega_0)^0$, vanish at $x = 0$ and in long-wave (or low-frequency) approximation has the $O[(\Omega\tau)^2]$ asymptotics. It is also straightforward to verify that both $g_\pm(x, t)$ and $w_\pm(x, t)$ are the pure imaginary values; sometimes it will be convenient to use the following approximate formulas:

$$1 + g_\pm(x, t) = 1 + i\Im[g_\pm(x, t)] \approx e^{i\Im[g_\pm(x, t)]}, \quad (5a)$$

$$1 + w_\pm(x, t) = 1 + i\Im[w_\pm(x, t)] \approx e^{i\Im[w_\pm(x, t)]}. \quad (5b)$$

III. RESPONSE OF A FABRY-PEROT CAVITY TO A PLANE GRAVITATIONAL WAVE

A. Input, circulating and output waves

Let us consider the operation of the optical scheme, illustrated in Fig. 1, which consists of platforms $P_{1,2}$ and a FP cavity assembled of two movable mirrors a and b , both lossless and having the amplitude transmission coefficient T , $|T| \ll 1$. We put distance between the mirrors in the absence of the gravitational wave and optical radiation to be equal to L . Without the loss of generality we assume the cavity to be lying in the plane $z = 0$ along one of the GW principal axes, coinciding with the x -axis.

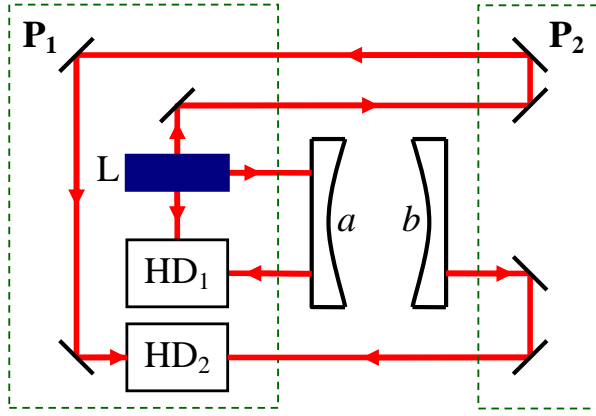


FIG. 1: Emission-detection scheme. Pump wave is radiated by laser L and reflected wave is detected with the homodyne detector HD₁. Transmitted wave is redirected towards platform P₁ and is detected with the homodyne detector HD₂. Laser L and both the homodyne detectors are assumed to be rigidly mounted on platform P₁. Mirrors which redirect the transmitted wave towards detector HD₂ are assumed to be rigidly mounted on platform P₂.

Laser L and the homodyne detectors HD_{1,2} are assumed to be *rigidly* mounted on platform P₁. In other words, we assume that all the elements on the platform do not move with respect to each other. Similarly, the auxiliary mirrors which redirect the transmitted wave (see below) are rigidly mounted on platform P₂. We introduce these requirements into our toy model in order not to deal with the inessential relative motions of the optical scheme elements. However, in practice these motions will result in some additional displacement noise.

In this section we will work in the proper reference frame of (the center of mass of) platform P₁ at which the origin of the coordinate system is set: $x_{P_1}(t) = 0$. Then the coordinates (their operators to be strict) of the mirrors are $x_a(t) = l_1 + X_a(t) \approx X_a(t)$ and $x_b(t) = L + l_1 + X_b(t) \approx L + X_b(t)$, where $l_1 \ll L$ is the negligible distance between the center of mass of platform P₁ and mirror a . The coordinate of (the center of mass of) platform P₂ is $x_{P_2}(t) = L + l_1 + l_2 + X_{P_2}(t) \approx L + X_{P_2}(t)$, where $l_2 \ll L$ is the negligible distance between the center of mass of platform P₂ and mirror b . Remind that $X_{a,b,P_2}(t)$ are the displacements with respect to non-inertial reference frame of platform P₁ and obey the relation $|X_{a,b,P_2}| \ll L$.

Let the cavity be pumped by laser L through mirror a with the input wave (see Fig. 2)

$$A_{\text{in}}(x, t) = A_{\text{in}0} \left[1 + g_+(x, t) + w_+(x, t) \right] e^{-i(\omega_1 t - k_1 x)} + a_{\text{in}}(x, t) e^{-i(\omega_1 t - k_1 x)}, \quad (6)$$

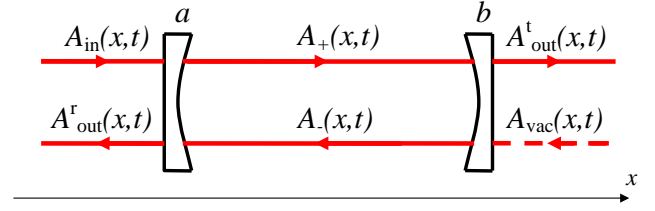


FIG. 2: Fabry-Perot cavity assembled of two movable mirrors a and b . Cavity is pumped through mirror a with the input wave $A_{\text{in}}(x, t)$ and through mirror b with the vacuum-state wave $A_{\text{vac}}(x, t)$. Optical field inside the cavity is represented as a sum of the wave $A_+(x, t)$, running in the positive direction of the x -axis, and the wave $A_-(x, t)$, running in the opposite direction. The reflection-output signal is $A_{\text{out}}^r(x, t)$ and transmission-output signal is $A_{\text{out}}^t(x, t)$.

and with the vacuum-state wave through mirror b :

$$A_{\text{vac}}(x, t) = a_{\text{vac}}(x, t) e^{-i[\omega_1 t + k_1(x-L)]}, \quad (7)$$

Here $a_{\text{in}}(x, t)$ is the “weak” field describing laser noise of the pump wave and $a_{\text{vac}}(x, t)$ is the “weak” field describing vacuum noise in the opposite input port. Remind, that both the laser and mirror a are located at $x \approx 0$, where $g(0, t) = w(0, t) = 0$, thus the input wave does not acquire distributed phase shift when it reaches mirror a .

It is convenient to represent the optical field inside the cavity as a sum of two waves, $A_+(x, t)$ and $A_-(x, t)$, running in the opposite directions:

$$A_{\pm}(x, t) = A_{\pm 0} \left[1 + g_{\pm}(x, t) + w_{\pm}(x, t) \right] e^{-i(\omega_1 t \mp k_1 x)} + a_{\pm}(x, t) e^{-i(\omega_1 t \mp k_1 x)}. \quad (8)$$

Here $a_{\pm}(x, t)$ describes the phase shift accumulated by the light wave while circulating inside the cavity.

Output wave reflected from the cavity is:

$$A_{\text{out}}^r(x, t) = A_{\text{out}0}^r \left[1 + g_-(x, t) + w_-(x, t) \right] e^{-i(\omega_1 t + k_1 x)} + a_{\text{out}}^r(x, t) e^{-i(\omega_1 t + k_1 x)}, \quad (9)$$

Quadrature components (see Appendix A) of this wave are assumed to be measured with the homodyne detector HD₁ (see Fig. 1). The reference oscillation is produced by laser L.

Output wave transmitted through the cavity

$$A_{\text{out}}^t(x, t) = A_{\text{out}0}^t \left[1 + g_+(x, t) + w_+(x, t) \right] e^{-i[\omega_1 t - k_1(x-L)]} + a_{\text{out}}^t(x, t) e^{-i[\omega_1 t - k_1(x-L)]}, \quad (10)$$

is redirected towards platform P₁ by the small auxiliary mirrors mounted on platform P₂. Quadratures of the transmitted wave are measured with the homodyne detector HD₂ (see Fig. 1). The reference oscillation is

produced by laser L which commits a single round trip along the $P_1 - P_2 - P_1$ path (see below).

Note that the complex amplitudes $a_{\text{out}}^{\text{r,t}}(x, t)$ are the unknown function of their arguments and are obtained as the solutions of the corresponding boundary problem for a FP cavity (see below). Obviously, they should vanish in the limit $R \rightarrow 0$, i.e. in the absence of the cavity, if $a_{\text{in}} = a_{\text{vac}} \equiv 0$. Therefore, below we call functions $a_{\text{out}}^{\text{r,t}}(x, t)$ or $a_{\text{out}}^{\text{r,t}}(\omega_1 + \Omega)$ the cavity response (or output) signals, meaning that they describe the influence of a FP cavity on the light propagation. The summand proportional to $A_{\text{out}0}^{\text{r}}$ in formula (9) and the one proportional to $A_{\text{out}0}^{\text{t}}$ in (10) thus correspond to the “no-cavity” case and are unimportant for us. In order to make our analysis more transparent we construct our detection scheme in such a way that these terms become unmeasurable.

In the case of reflected wave both $g_-(x, t)$ and $w_-(x, t)$ vanish at $x = 0$ and the only measurable quantities left are the quadratures of $a_{\text{out}}^{\text{r}}(x, t)$.

The case of transmitted wave is more complex. Note that the $A_{\text{out}0}^{\text{t}}$ -summand in formula (10) at point $x = x_{P_2}(t)$ describes a *single* forward trip of light along the cavity:

$$\begin{aligned} & \left[1 + g_+(x_{P_2}, t) + w_+(x_{P_2}, t) \right] e^{ik_1 X_{P_2}(t)} \\ & \approx \exp \left\{ ik_1 X_{P_2}(t) + i\mathcal{J} \left[g_+(L, t) + w_+(L, t) \right] \right\}. \end{aligned}$$

Here we used formulas (5a) and (5b). Remind also, that the transmitted wave is redirected towards platform P_1 for detection and thus commits a backward trip. Clearly, the whole round trip will result in phase shift

$$2k_1 X_{P_2}(t) + \mathcal{J} \left[g_+(L, t) - g_-(L, t) + w_+(L, t) - w_-(L, t) \right].$$

In order to make this phase shift unmeasurable we make

the reference wave, produced by laser L, to travel the same round trip before returning to the homodyne detector HD₂. Ultimately, both the additional phases of the transmitted wave and of the reference oscillation are completely subtracted in the homodyne measurement. Therefore, the only measurable quantities left in the transmitted wave are the quadratures of $a_{\text{out}}^{\text{t}}(x, t)$.

It is worth noting that such a detection scheme only serves a purpose of making the analysis of our toy model more transparent; it may be hard to justify its implementation in practice.

B. Response signals of a Fabry-Perot cavity

To obtain the response functions of a Fabry-Perot cavity we substitute fields (6 – 10) into the set of boundary conditions (conditions of the electric field continuity along the surfaces of the mirrors) [37, 53]:

$$A_+(x_a, t) = TA_{\text{in}}(x_a, t) - RA_-(x_a, t), \quad (11a)$$

$$A_{\text{out}}^{\text{r}}(x_a, t) = RA_{\text{in}}(x_a, t) + TA_-(x_a, t), \quad (11b)$$

$$A_-(x_b, t) = TA_{\text{vac}}(x_b, t) - RA_+(x_b, t), \quad (11c)$$

$$A_{\text{out}}^{\text{t}}(x_b, t) = RA_{\text{vac}}(x_b, t) + TA_+(x_b, t). \quad (11d)$$

This set of equations is accurate up to the 0th order of Ω/ω_1 since it does not take into account the relativistic terms proportional to $\dot{X}_{a,b}/c$ [37]. The solution of this set is obtained in Appendix B using the method of successive approximations. Since we do not consider the effect of parametric excitation of the additional optical modes under the influence of the GW [37], it will be convenient to introduce the detuning $\delta_1 = \omega_1 - \pi n_0/\tau$, where n_0 is integer, even (for simplicity) and fixed; $\tau = L/c$. Then the solution of the 1st order takes the following form (all spectral arguments are omitted):

$$a_{\text{out}}^{\text{r}} = \frac{R - Re^{2i(\delta_1 + \Omega)\tau}}{1 - R^2 e^{2i(\delta_1 + \Omega)\tau}} a_{\text{in}} + \frac{T^2 e^{i(\delta_1 + \Omega)\tau}}{1 - R^2 e^{2i(\delta_1 + \Omega)\tau}} a_{\text{vac}} - \frac{RT^2 A_{\text{in}0} e^{2i\delta_1\tau}}{1 - R^2 e^{2i\delta_1\tau}} i \frac{2k_1(X_b e^{i\Omega\tau} - \sigma_1 X_a) + \delta\Psi_{\text{emw}}}{1 - R^2 e^{2i(\delta_1 + \Omega)\tau}}, \quad (12a)$$

$$a_{\text{out}}^{\text{t}} = \frac{T^2 e^{i(\delta_1 + \Omega)\tau}}{1 - R^2 e^{2i(\delta_1 + \Omega)\tau}} a_{\text{in}} + \frac{R - Re^{2i(\delta_1 + \Omega)\tau}}{1 - R^2 e^{2i(\delta_1 + \Omega)\tau}} a_{\text{vac}} + \frac{RT^2 A_{\text{in}0} e^{3i\delta_1\tau}}{1 - R^2 e^{2i\delta_1\tau}} i \frac{2k_1(X_b e^{i\Omega\tau} - X_a) + \delta\Psi_{\text{emw}}}{1 - R^2 e^{2i(\delta_1 + \Omega)\tau}} e^{i\Omega\tau}. \quad (12b)$$

Here phase shift $\delta\Psi_{\text{emw}} = \delta\Psi_{\text{gw+emw}} + \delta\Psi_{\text{acc+emw}}$, calculated in the approximation $\Omega/\omega_1 \ll 1$, describes the direct coupling of the optical wave to the GW and acceleration fields:

$$\delta\Psi_{\text{gw+emw}}(\Omega) = -k_1 L h(\Omega) \left(1 - \frac{\sin \Omega\tau}{\Omega\tau} \right) e^{i\Omega\tau}, \quad (13a)$$

$$\delta\Psi_{\text{acc+emw}}(\Omega) = -k_1 \xi_{P_1}(\Omega) \left(1 - 2e^{i\Omega\tau} + e^{2i\Omega\tau} \right). \quad (13b)$$

Remind that $\xi_{P_1}(\Omega)$ is the fluctuative displacement of platform P_1 measured in the laboratory frame. Factor

$$\begin{aligned} \sigma_1(\Omega) &= e^{-2i\delta_1\tau} / T^2 \\ &\times \left[1 - R^2 e^{2i\delta_1\tau} - R^2 e^{2i(\delta_1 + \Omega)\tau} + R^2 e^{2i(2\delta_1 + \Omega)\tau} \right], \end{aligned}$$

describes the difference between $a_{\text{out}}^{\text{r}}$ and $a_{\text{out}}^{\text{t}}$, playing the key role in our further consideration. In the resonant regime ($\delta_1 = 0$) we have $\sigma_1 = 1$, thus it is convenient to

rewrite factor σ_1 as a sum $1 + \Delta\sigma_1$, where:

$$\Delta\sigma_1 = (1 - e^{2i\delta_1\tau}) \frac{1 - R^2 e^{2i(\delta_1+\Omega)\tau}}{T^2} e^{-2i\delta_1\tau},$$

Remind also, that the transmitted wave is redirected towards platform P_1 for detection. Therefore, the truly measured quantity is $a_{\text{out}}^t e^{i(\delta_1+\Omega)\tau}$. However, keeping this in mind, below we deal only with a_{out}^t . The additional phase can be taken into account straightforwardly.

We should now express the obtained result in terms of (i) the fluctuative displacements measured in the laboratory frame and (ii) the GW displacement measured in the local Lorentz frame of platform P_1 . According to formula (2) the transformation law is:

$$X_a(t) = \xi_a(t) - \xi_{P_1}(t), \quad (14a)$$

$$X_b(t) = \frac{1}{2} Lh(t) + \xi_b(t) - \xi_{P_1}(t). \quad (14b)$$

Here we denoted the fluctuative motions of mirrors a and b as $\xi_{a,b}$. These formulas are strict for any separation between the mirrors. Substituting X_a and X_b into the response signals (12a) and (12b) we rewrite them in terms of the GW signal

$$\xi_{\text{gw}}(\Omega) = \frac{1}{2} Lh(\Omega) \frac{\sin \Omega\tau}{\Omega\tau},$$

and fluctuating displacements ξ_{a,b,P_1} :

$$\begin{aligned} a_{\text{out}}^r &= \mathcal{R}_1 a_{\text{in}} + \mathcal{T}_1 a_{\text{vac}} \\ &- \frac{RT^2 A_{\text{in}0} e^{2i\delta_1\tau}}{\mathcal{T}_{\delta_1}^2 \mathcal{T}_{\delta_1+\Omega}^2} 2ik_1 \left[\xi_b e^{i\Omega\tau} - \sigma_1 \xi_a + \xi_{\text{gw}} e^{i\Omega\tau} \right] \\ &- \frac{RT^2 A_{\text{in}0} e^{2i\delta_1\tau}}{\mathcal{T}_{\delta_1}^2 \mathcal{T}_{\delta_1+\Omega}^2} ik_1 \xi_{P_1} (2\sigma_1 - 1 - e^{2i\Omega\tau}), \end{aligned} \quad (15a)$$

$$\begin{aligned} a_{\text{out}}^t &= \mathcal{T}_1 a_{\text{in}} + \mathcal{R}_1 a_{\text{vac}} \\ &+ \frac{R^2 T^2 A_{\text{in}0} e^{3i\delta_1\tau}}{\mathcal{T}_{\delta_1}^2 \mathcal{T}_{\delta_1+\Omega}^2} 2ik_1 \left[\xi_b e^{i\Omega\tau} - \xi_a + \xi_{\text{gw}} e^{i\Omega\tau} \right] e^{i\Omega\tau} \\ &+ \frac{R^2 T^2 A_{\text{in}0} e^{3i\delta_1\tau}}{\mathcal{T}_{\delta_1}^2 \mathcal{T}_{\delta_1+\Omega}^2} ik_1 \xi_{P_1} (1 - e^{2i\Omega\tau}) e^{i\Omega\tau}. \end{aligned} \quad (15b)$$

The following notations have been introduced above:

$$\begin{aligned} \mathcal{T}_{\delta_1}^2 &= 1 - R^2 e^{2i\delta_1\tau}, & \mathcal{T}_{\delta_1+\Omega}^2 &= 1 - R^2 e^{2i(\delta_1+\Omega)\tau}, \\ \mathcal{R}_1 &= \frac{R - R e^{2i(\delta_1+\Omega)\tau}}{1 - R^2 e^{2i(\delta_1+\Omega)\tau}}, & \mathcal{T}_1 &= \frac{T^2 e^{i(\delta_1+\Omega)\tau}}{1 - R^2 e^{2i(\delta_1+\Omega)\tau}}, \end{aligned}$$

having the following physical meaning: $1/\mathcal{T}_{\delta_1}^2$ describes the resonant amplification of the input amplitude $A_{\text{in}0}$ inside the cavity, $1/\mathcal{T}_{\delta_1+\Omega}^2$ describes the frequency-dependent resonant amplification of the variation of the circulating light wave, \mathcal{R}_1 and \mathcal{T}_1 are the generalized coefficients of reflection (from a FP cavity) and transmission (through a FP cavity).

It is convenient to consider the physical meaning of the obtained formulas. First we analyze the reflected wave rewriting it in the following form:

$$a_{\text{out}}^r = \mathcal{R}_1 (a_{\text{in}} - A_{\text{in}0} ik_1 \xi_{P_1}) + \mathcal{T}_1 a_{\text{vac}}$$

$$\begin{aligned} &+ TA_{-0} 2ik_1 \left[(\xi_b + \xi_{\text{gw}}) e^{i\Omega\tau} - \xi_a \right] / \mathcal{T}_{\delta_1+\Omega}^2 \\ &+ A_{\text{out}0} 2ik_1 \xi_a - A_{\text{out}0} ik_1 \xi_{P_1}. \end{aligned}$$

The 1st term states that the optical laser noise a_{in} is indistinguishable from laser displacement noise ξ_{P_1} , so they always come together. The 2nd summand describes the propagation of the vacuum noise through a FP cavity. The 3rd term is the light wave flowing out of the cavity containing the accumulated phase shift. The 4th summand, which is responsible for $\Delta\sigma_1$, describes the prompt reflection from the input mirror a . The last term describes the phase shift acquired by the light wave due to displacement noise of detector on platform P_1 .

In a similar way one can consider the transmitted wave. The only difference which should be taken into account is the following: the term proportional to ξ_{P_1} in formula (15b) cannot be reduced to $-\mathcal{T}_1 A_{\text{in}0} ik_1 \xi_{P_1}$ due to the detection scheme we use for the transmitted wave. If one adds the $A_{\text{out}0}^t$ -summand in formula (10) to a_{out}^t then $-\mathcal{T}_1 A_{\text{in}0} ik_1 \xi_{P_1}$ is recovered.

IV. DOUBLE-PUMPED FABRY-PEROT CAVITY

A. Response signals of a double-pumped Fabry-Perot cavity

Let a single Fabry-Perot cavity be pumped through both of its mirrors (see Fig. 3). We assume the pump wave through mirror a to have amplitude \mathcal{A} , detuning δ_1 (carrier frequency ω_1), polarization in the plane of incidence and denote it with A_{in} ; the pump wave through mirror b is assumed to have amplitude \mathcal{B} , detuning δ_2 (carrier frequency ω_2), polarization orthogonal to the plane of incidence and is denoted with B_{in} . Corresponding vacuum pumps through mirrors b and a are denoted with A_{vac} and B_{vac} .

The response functions corresponding to the pump through mirror b are straightforwardly obtained from functions (15a, 15b) replacing $\delta_1 \rightarrow \delta_2$, $\xi_a \rightarrow -\xi_b$, $\xi_b \rightarrow -\xi_a$, $\xi_{P_1} \rightarrow -\xi_{P_2}$ and keeping the GW term unchanged due to the symmetry of the system and plane GW wavefront. For convenience we gather signals in all the four output ports of the DFPF cavity omitting spectral arguments and taking into account the relation $k_1 \approx k_2 \equiv k_0$ valid for the corresponding carrier frequencies ω_1 and ω_2 lying within the same resonance curve:

$$\begin{aligned} a_{\text{out}}^r &= \mathcal{R}_1 a_{\text{in}} + \mathcal{T}_1 a_{\text{vac}} \\ &- \frac{RT^2 \mathcal{A} e^{2i\delta_1\tau}}{\mathcal{T}_{\delta_1}^2 \mathcal{T}_{\delta_1+\Omega}^2} 2ik_0 \left[(\xi_b + \xi_{\text{gw}}) e^{i\Omega\tau} - \sigma_1 \xi_a \right] \\ &- \frac{RT^2 \mathcal{A} e^{2i\delta_1\tau}}{\mathcal{T}_{\delta_1}^2 \mathcal{T}_{\delta_1+\Omega}^2} ik_0 \xi_{P_1} (2\sigma_1 - 1 - e^{2i\Omega\tau}), \quad (16a) \\ a_{\text{out}}^t &= \mathcal{T}_1 a_{\text{in}} + \mathcal{R}_1 a_{\text{vac}} \end{aligned}$$

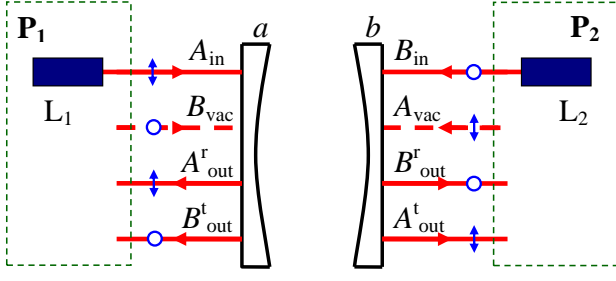


FIG. 3: Fabry-Perot cavity pumped through both of its mirrors (a DPFP cavity). Lasers L_1 and L_2 are rigidly mounted on platforms P_1 and P_2 respectively. The pump wave through mirror a is denoted with A_{in} and is assumed to be polarized in the plane of incidence. The pump wave through mirror b is denoted with B_{in} and is assumed to be polarized normally to the plane of incidence. Corresponding vacuum pumps are A_{vac} and B_{vac} . Output ports are $A_{\text{out}}^{\text{r,t}}$.

$$+ \frac{R^2 T^2 \mathcal{A} e^{3i\delta_1 \tau}}{\mathcal{T}_{\delta_1}^2 \mathcal{T}_{\delta_1 + \Omega}^2} 2ik_0 \left[(\xi_b + \xi_{\text{gw}}) e^{2i\Omega\tau} - \xi_a e^{i\Omega\tau} \right] + \frac{R^2 T^2 \mathcal{A} e^{3i\delta_1 \tau}}{\mathcal{T}_{\delta_1}^2 \mathcal{T}_{\delta_1 + \Omega}^2} ik_0 \xi_{P_1} (1 - e^{2i\Omega\tau}) e^{i\Omega\tau}, \quad (16b)$$

$$b_{\text{out}}^{\text{r}} = \mathcal{R}_2 b_{\text{in}} + \mathcal{T}_2 b_{\text{vac}} - \frac{RT^2 \mathcal{B} e^{2i\delta_2 \tau}}{\mathcal{T}_{\delta_2}^2 \mathcal{T}_{\delta_2 + \Omega}^2} 2ik_0 \left[(-\xi_a + \xi_{\text{gw}}) e^{i\Omega\tau} + \sigma_2 \xi_b \right] + \frac{RT^2 \mathcal{B} e^{2i\delta_2 \tau}}{\mathcal{T}_{\delta_2}^2 \mathcal{T}_{\delta_2 + \Omega}^2} ik_0 \xi_{P_2} (2\sigma_2 - 1 - e^{2i\Omega\tau}), \quad (16c)$$

$$b_{\text{out}}^{\text{t}} = \mathcal{T}_2 b_{\text{in}} + \mathcal{R}_2 b_{\text{vac}} + \frac{R^2 T^2 \mathcal{B} e^{3i\delta_2 \tau}}{\mathcal{T}_{\delta_2}^2 \mathcal{T}_{\delta_2 + \Omega}^2} 2ik_0 \left[(-\xi_a + \xi_{\text{gw}}) e^{2i\Omega\tau} + \xi_b e^{i\Omega\tau} \right] - \frac{R^2 T^2 \mathcal{B} e^{3i\delta_2 \tau}}{\mathcal{T}_{\delta_2}^2 \mathcal{T}_{\delta_2 + \Omega}^2} ik_0 \xi_{P_2} (1 - e^{2i\Omega\tau}) e^{i\Omega\tau}. \quad (16d)$$

Here quantities \mathcal{R} , \mathcal{T} , \mathcal{T}_{δ}^2 and $\mathcal{T}_{\delta+\Omega}^2$ with the subscripts “1” and “2” are evaluated for detunings δ_1 and δ_2 correspondingly.

The quadrature components of field amplitudes (16c) and (16d) can be measured in a way similar to the case of a single-pumped FP cavity (corresponding to field amplitudes (16a) and (16b)). The detection scheme of a DPFP cavity will require two more homodyne detectors to measure the output signals corresponding to the second pump.

B. Cancellation of displacement noise

Now we will demonstrate the noise cancellation from the combination of field amplitudes (16a – 16d). Though it is obvious and enough from the theoretical point of view, such a consideration is surely insufficient for the

experimental purposes, because we can only measure quadrature components of the fields, not the complex field amplitudes themselves. However, we will not present the bulky calculations of the quadratures here since we consider only the toy model, not the experimental design.

Therefore, let us assume that we are able to produce any desired linear combination of the response signals (16a – 16d). Physically this means that we are able to construct a set of optical lossless filters with the predetermined transmittance coefficients, transmit each wave through its filter and then make the waves interfere.

To illustrate our method of noise elimination we will construct the linear combination of responses which cancels fluctuating displacements $\xi_{a,b}$ in three steps. Remind that the transmitted signals do not take into account the $e^{i(\delta_1 + \Omega)\tau}$ multiplier.

From the first pair of signals $a_{\text{out}}^{\text{r,t}}$ we can eliminate either ξ_a or $\xi_b + \xi_{\text{gw}}$. Let us cancel ξ_a . Multiplying $a_{\text{out}}^{\text{r}}$ on $Re^{i(\delta_1 + \Omega)\tau}$ and adding it to $\sigma_1 a_{\text{out}}^{\text{t}}$ we obtain:

$$s_1 = Re^{i(\delta_1 + \Omega)\tau} a_{\text{out}}^{\text{r}} + \sigma_1 a_{\text{out}}^{\text{t}} = s_1^{\text{fl}} + \frac{R^2 T^2 \mathcal{A} e^{3i\delta_1 \tau}}{\mathcal{T}_{\delta_1}^2 \mathcal{T}_{\delta_1 + \Omega}^2} 2ik_0 \Delta\sigma_1 (\xi_b + \xi_{\text{gw}}) e^{2i\Omega\tau} - \frac{R^2 T^2 \mathcal{A} e^{3i\delta_1 \tau}}{\mathcal{T}_{\delta_1}^2 \mathcal{T}_{\delta_1 + \Omega}^2} ik_0 \Delta\sigma_1 \xi_{P_1} (1 + e^{2i\Omega\tau}) e^{i\Omega\tau} = s_1^{\text{fl}} + R^2 e^{i\delta_1 \tau} (1 - e^{2i\delta_1 \tau}) \frac{\mathcal{A}}{\mathcal{T}_{\delta_1}^2} 2ik_0 (\xi_b + \xi_{\text{gw}}) e^{2i\Omega\tau} - R^2 e^{i\delta_1 \tau} (1 - e^{2i\delta_1 \tau}) \frac{\mathcal{A}}{\mathcal{T}_{\delta_1}^2} ik_0 \xi_{P_1} (1 + e^{2i\Omega\tau}) e^{i\Omega\tau}, \quad (17)$$

$$s_1^{\text{fl}} = a_{\text{in}} e^{-i(\delta_1 - \Omega)\tau} + \frac{R}{T^2} \left[e^{2i\Omega\tau} (e^{2i\delta_1 \tau} - 1) + \mathcal{T}_{\delta_1}^2 e^{-2i\delta_1 \tau} \right] a_{\text{vac}}.$$

Similarly, from the second pair of signals $b_{\text{out}}^{\text{r,t}}$ we can eliminate either ξ_b or $-\xi_a + \xi_{\text{gw}}$. Since we have already canceled ξ_a from the first pair and are left only with $\xi_b + \xi_{\text{gw}}$, we need to exclude $-\xi_a + \xi_{\text{gw}}$ from the second pair to be left with ξ_b only. Multiplying $b_{\text{out}}^{\text{r}}$ on $Re^{i(\delta_2 + \Omega)\tau}$ and adding it to $b_{\text{out}}^{\text{t}}$ we obtain:

$$s_2 = Re^{i(\delta_2 + \Omega)\tau} b_{\text{out}}^{\text{r}} + b_{\text{out}}^{\text{t}} = s_2^{\text{fl}} - \frac{R^2 T^2 \mathcal{B} e^{3i\delta_2 \tau}}{\mathcal{T}_{\delta_2}^2 \mathcal{T}_{\delta_2 + \Omega}^2} 2ik_0 \Delta\sigma_2 (\xi_b - \xi_{P_2}) e^{i\Omega\tau} = s_2^{\text{fl}} - R^2 e^{i\delta_2 \tau} (1 - e^{2i\delta_2 \tau}) \frac{\mathcal{B}}{\mathcal{T}_{\delta_2}^2} 2ik_0 (\xi_b - \xi_{P_2}) e^{i\Omega\tau}, \quad (18)$$

$$s_2^{\text{fl}} = b_{\text{in}} e^{i(\delta_2 + \Omega)\tau} + R b_{\text{vac}}.$$

To perform the last step we need to introduce the relation between \mathcal{A} and \mathcal{B} . It is convenient (but not necessary) to assume $\mathcal{A}/\mathcal{T}_{\delta_1}^2 = \mathcal{B}/\mathcal{T}_{\delta_2}^2$. Ultimately we cancel

the information about ξ_b from the pair of signals $s_{1,2}$:

$$\begin{aligned}
s &= s_1 + \frac{e^{i\delta_1\tau}(1 - e^{2i\delta_1\tau})}{e^{i\delta_2\tau}(1 - e^{2i\delta_2\tau})} s_2 e^{i\Omega\tau} \\
&= s^{\text{fl}} + R^2 e^{i(\delta_1+\Omega)\tau} (1 - e^{2i\delta_1\tau}) \frac{\mathcal{A}}{\mathcal{T}_{\delta_1}^2} \\
&\quad \times ik_0 \left[-\xi_{P_1} + 2(\xi_{P_2} + \xi_{\text{gw}}) e^{i\Omega\tau} - \xi_{P_1} e^{2i\Omega\tau} \right], \quad (19) \\
s^{\text{fl}} &= a_{\text{in}} e^{-i(\delta_1-\Omega)\tau} + \frac{1 - e^{2i\delta_1\tau}}{1 - e^{2i\delta_2\tau}} b_{\text{in}} e^{i(\delta_1+2\Omega)\tau} \\
&\quad + \frac{R}{\mathcal{T}^2} \left[e^{2i\Omega\tau} (e^{2i\delta_1\tau} - 1) + \mathcal{T}_{\delta_1}^2 e^{-2i\delta_1\tau} \right] a_{\text{vac}} \\
&\quad + \frac{e^{i\delta_1\tau}(1 - e^{2i\delta_1\tau})}{e^{i\delta_2\tau}(1 - e^{2i\delta_2\tau})} R b_{\text{vac}} e^{i\Omega\tau}.
\end{aligned}$$

The total signal s , below called DFI response signal, does not contain information about displacement noise of the mirrors but is not free from displacement noise of the platforms.

For the ground-based detectors with the spacial scale L of several kilometers the most important is the low-frequency response, i.e. the limit $\Omega L/c \ll 1$. We will analyze two special cases.

In the simplest case of equal pumps we have $\mathcal{A} = \mathcal{B}$ and $\delta_1 = \delta_2$. Then in the narrow-band approximation ($T^2 = 2\gamma\tau \ll 1$, $\delta_{1,2}\tau \ll 1$, where γ is the cavity half-bandwidth):

$$\begin{aligned}
s|_{\delta_2=\delta_1} &\approx a_{\text{in}} + b_{\text{in}} + a_{\text{vac}} + b_{\text{vac}} \\
&\quad - \frac{i\delta_1}{\gamma - i\delta_1} \mathcal{A} 2ik_0 \left(\frac{1}{2} Lh + \xi_{P_2} - \xi_{P_1} \right). \quad (20)
\end{aligned}$$

Remind [40, 41, 42, 43, 44], that due to the significant amplification of the input laser power inside a FP cavity test masses are subjected to the force of radiation pressure. It is known that the sign of the induced ponderomotive rigidity depends on the sign of detuning. Therefore, in order to cancel the effects of radiation pressure we should consider the pumps with opposite detunings $\delta_2 = -\delta_1$. In this case both the pumps create ponderomotive rigidities with opposite signs and the total rigidity vanishes. The DFI signal in this case is:

$$\begin{aligned}
s|_{\delta_2=-\delta_1} &\approx a_{\text{in}} - b_{\text{in}} + a_{\text{vac}} - b_{\text{vac}} \\
&\quad - \frac{i\delta_1}{\gamma - i\delta_1} \mathcal{A} 2ik_0 \left(\frac{1}{2} Lh + \xi_{P_2} - \xi_{P_1} \right). \quad (21)
\end{aligned}$$

Obviously, in the previous case of equal detunings total ponderomotive rigidity does not vanish and, strictly speaking, the effects of radiation pressure in the DFPF cavity require detailed analysis.

From the formulas (20) and (21) we conclude that the signal-to-noise ratio of the DFPF cavity operating as the displacement-noise-free detector is of the same order as for the configuration with two test masses and only one round trip of light between them (i.e. without the resonant gain).

V. DISCUSSION

A. Physical mechanism of noise cancelation

Relying on the results of the previous sections we may now consider a simplified mathematical model of a FP cavity and discuss the physical mechanism underlying the noise elimination algorithm.

Formulas (15a, 15b) in the $\Omega\tau \ll 1$ limit can be derived from the intuitive reasonings. It is evident that the circulating wave inside the cavity measures the relative displacement of mirrors a and b plus GW displacement: $\xi_{\text{gw}} + \xi_b - \xi_a$. Transmitted signal, measured as illustrated in Fig. 1, is directly proportional to this quantity:

$$a_{\text{out}}^t = q_1 (\xi_{\text{gw}} + \xi_b - \xi_a), \quad (22)$$

where q_1 includes the frequency-dependent resonant multiplier $1/\mathcal{T}_{\delta_1+\Omega}^2$. The reflected signal is somewhat different: it also includes the component due to the prompt reflection of the pump wave from the input mirror. For instance, if the cavity is pumped through mirror a then this component is proportional to $\xi_a - \xi_{P_1}$. The reflected signal is then

$$a_{\text{out}}^r = p(\xi_a - \xi_{P_1}) + q_2(\xi_{\text{gw}} + \xi_b - \xi_a). \quad (23)$$

Here q_2 is also proportional to $1/\mathcal{T}_{\delta_1+\Omega}^2$. Equations (22) and (23) tell us that we are unable to measure absolute values of ξ_a and ξ_b , only relative measurements with respect to detectors (platform P_1) are allowed.

The second pair of pumps can be derived in full similarity. Let us consider the simplest case of equal pumps. Then due to the symmetry of the system and plane GW wavefront the second pair of responses can be written as:

$$\begin{aligned}
b_{\text{out}}^t &= q_1 (\xi_{\text{gw}} + \xi_b - \xi_a), \\
b_{\text{out}}^r &= p(\xi_{P_2} - \xi_b) + q_2 (\xi_{\text{gw}} + \xi_b - \xi_a).
\end{aligned}$$

Here displacements of the mirrors are measured with respect to platform P_2 .

Now constructing the following linear combination of the responses

$$s = a_{\text{out}}^r + \frac{p - q_2}{q_1} a_{\text{out}}^t + b_{\text{out}}^r - \frac{q_2}{q_1} b_{\text{out}}^t,$$

we are able to cancel displacement noise of both the mirrors but not the one of the platforms:

$$s = p(\xi_{\text{gw}} + \xi_{P_2} - \xi_{P_1}). \quad (24)$$

This is the direct consequence of the relativity principle which states that no absolute coordinate and velocity measurements are allowed. According to formula (24), noise cancelation in the DFPF cavity is possible due to the effect of prompt reflection from the input mirror. The obtained DFI response is similar to the response of a simple single-pass GW detector: an observer sends the light

wave to the reflective mirror and receives it back measuring the phase shift. The noise-cancellation algorithm that we perform for a DPFP cavity in some sense can be interpreted as removal of the cavity “by hands”. Evidently, this results in the loss of the optical resonant gain: signal s in formula (24) includes neither q_1 nor q_2 .

In conventional (LIGO) topology both the mean amplitude and the signal are resonantly amplified resulting in less power needed to reach the SQL level of sensitivity. For instance, in Advanced LIGO detectors (utilizing also the power recycling mirrors) SQL will be reached with ≈ 1 MW of circulating optical power corresponding to ≈ 100 W laser. In contrast, in a DPFP cavity the same level of sensitivity will be reached at ≈ 1 GW of laser power. This number might not seem so dramatic if one reminds that the squeezed light allows to decrease the power needed. To achieve the high factors of squeezing one must provide the mirrors with the coefficient of optical losses as small as possible; according to J.M. Makowsky there is a strong evidence that the loss coefficient $\sim 10^{-9}$ will be reached in near future.

Two special cases when noise cancellation is impossible are worth noting.

1. Resonant pump. One can derive from formula (15a) that the coefficient p is proportional to the amplitude of reflected wave $A_{\text{out}0}$. In Appendix B it is found that $A_{\text{out}0} = RA_{\text{in}0}(1 - e^{2i\delta_1\tau})/T_{\delta_1}^2$. Thus in the resonant regime ($\delta_1 = 0$) reflected wave has no “strong” component meaning that the prompt reflection from the input mirror does not occur and $p = 0$. As a result, both the reflected and transmitted signals become indistinguishable, i.e. they carry equal amount of information about the coordinates of the mirrors (see equations (22) and (23)). In general case (formulas (15a) and (15b)) the resonant regime corresponds to $\Delta\sigma_1 = 0$, resulting in the relation $a_{\text{out}}^t = -Ra_{\text{out}}^r e^{i\Omega\tau}$, neglecting the optical noise.
2. Mirrors mounted on the platforms. One may think of mounting the mirrors on the platforms to reduce the additional fluctuative degrees of freedom associated with the platforms. For instance, if the mirror a is mounted on platform P_1 then $\xi_a = \xi_{P_1}$ and from equation (23) it is evident that both the responses become equivalent. In general case (see formulas (12a) and (12b)) it is evident that for $X_a = \xi_a - \xi_{P_1} = 0$ again $a_{\text{out}}^t = -Ra_{\text{out}}^r e^{i\Omega\tau}$. This fact is the direct illustration of the theorem proved in Ref. [28]: no *complete* displacement-noise cancellation is possible in a one-dimensional system.

Remind that $\xi_{\text{gw}} \approx Lh/2$ so direct coupling of the GW to the light wave plays no role in our noise-cancellation scheme. From the reasonings above we may now conclude that it is hardly possible (without contradicting the relativity principle) to completely eliminate the displacement noise, keeping simultaneously the $h(L/\lambda_{\text{gw}})^0$ or

$h(L/\lambda_{\text{gw}})^1$ order of the DFI signal, since these orders correspond to coordinate and velocity measurements. Only acceleration, in principle, can be measured absolutely, corresponding to the true DFI of the $h(L/\lambda_{\text{gw}})^n$, $n \geq 2$ order proposed by Kawamura *et al.* Thus we are left to choose either sacrifice with the GW sensitivity but completely eliminate displacement noise, or keep good GW sensitivity at the expense of incomplete noise cancellation. To suppress the fluctuations associated with the platforms (where lasers and detectors are mounted) one will need to increase their masses and cool them down to cryogenic temperatures. The only limiting factors will be left then are the classical (laser) and vacuum optical noises.

B. Further prospects: cancelation of laser noise and detection schemes

In practice laser noise dominates over vacuum shot noise. In addition, as pointed out in Ref. [28], optical laser noise is indistinguishable from laser displacement noise. Therefore, in order to increase the SNR of the DPFP cavity we should somehow eliminate the laser noise. Several obvious DPFP-based laser-noise-cancellation schemes can be proposed [54]: (i) with a single DPFP cavity where both the pumps are generated with a single laser and one of the pumps is redirected towards mirror b via additional optical path, (ii) with a pair of parallel and closely located DPFP cavities having different bandwidths and/or detunings, (iii) modification of the conventional LIGO Michelson/Fabry-Perot topology, etc. However, the major drawback of all such schemes is the significant amount of the additional optical elements such as beamsplitters and mirrors which are utilized to split and redirect laser beams. These elements introduce the additional displacement noise with the magnitude compared to the GW signal $k_0 Lh$. In conventional interferometers (such as LIGO) this additional noise is negligible as compared to the finesse times amplified GW signal (and mirrors displacement noise), while the DPFP cavity operating in the DFI regime effectively “loses” the resonant gain as discussed in Sec. V A. Therefore, the problem of additional displacement noise requires a separate detailed analysis and it may turn out that it will be highly suppressed after performing the noise-cancellation algorithm described in Sec. IV B.

The related problem is the construction of the experimentally viable and most practical measurement schemes. In particular, in this paper we assumed all the optical elements (lasers, detectors, auxiliary mirrors) on platforms P_1 and P_2 to be noiseless (i.e. rigidly mounted). In practice this assumption may be hard to justify and thus requires further intensive study. Moreover, the detection scheme for transmitted wave considered in this paper seems quite unnatural from the experimental point of view and its implementation may also be complicated in practice. Thus other configurations

of detection scheme should be analyzed. One may find use of the amplitude detectors instead of the homodyne detectors.

VI. CONCLUSION

In this paper we have analyzed the operation of a Fabry-Perot cavity pumped through both the mirrors (a DFPF cavity) performing the mirrors-displacement-noise-free gravitational-wave detection. We have demonstrated that due to the asymmetry between the reflection and transmission output ports of detuned cavity it is possible to construct a linear combination of four response signals which cancels displacement fluctuations of the mirrors. At low frequencies the GW response of the DFPF cavity turns out to be far better than that of the Mach-Zehnder-based DFIs proposed by S. Kawamura *et al.* due to the different mechanisms of noise-cancellation. However, the effective loss of the resonant gain results in the sensitivity limitation of the DFPF cavity by displacement noise of lasers and detectors.

The performed analysis suggests that the DFPF cavity can be considered a promising candidate for the future generation GW detector prototype, provided the noises of lasers and detectors are suppressed: it allows the significant extension of the frequency band of the ground-based detectors and by elimination of the back-action noise straightforwardly avoids the standard quantum limitation.

The problems of (i) DFPF-based laser-noise-cancellation schemes, (ii) viable measurement schemes and (iii) radiation pressure effects in a DFPF cavity require future investigation.

Acknowledgments

We would like to thank V.B. Braginsky, M.L. Gorodetsky and F.Ya. Khalili for fruitful discussions and valuable critical remarks on the paper. We are very grateful to T. Corbitt for his suggestions about the improvement of the text. In particular, we would like to express our gratitude to Y. Chen for the hospitality and support during our stay at AEI and the inspiring discussions which greatly helped to improve our research. This work was supported by LIGO team from Caltech and in part by NSF and Caltech grant PHY-0353775 and by Grant of President of Russian Federation NS-5178.2006.2.

APPENDIX A: QUANTIZED ELECTROMAGNETIC WAVE

In this Appendix we introduce the notations for the quantized field of electromagnetic wave which will be used throughout the paper.

In quantum electrodynamics the operator of electric field in Heisenberg picture is:

$$A(x, t) = \int_0^\infty \sqrt{\frac{2\pi\hbar\omega}{Sc}} a(\omega) e^{-i\omega(t-x/c)} \frac{d\omega}{2\pi} + \text{h.c.},$$

where S is the effective cross section area of the laser beam and $a(\omega)$ is the annihilation operator obeying the commutation relations

$$[a(\omega), a(\omega')] = 0, \quad [a(\omega), a^\dagger(\omega')] = 2\pi\delta(\omega - \omega').$$

It will be convenient now to introduce the carrier frequency ω_0 : $\omega = \omega_0 + \Omega$, $|\Omega| \ll \omega_0$, and to rewrite the field operator in the following way:

$$\begin{aligned} A(x, t) &= e^{-i(\omega_0 t - k_0 x)} \\ &\times \int_{-\omega_0}^\infty \sqrt{\frac{2\pi\hbar(\omega_0 + \Omega)}{Sc}} a(\omega_0 + \Omega) e^{-i\Omega(t-x/c)} \frac{d\Omega}{2\pi} \\ &+ \text{h.c.}, \end{aligned}$$

where $k_0 = \omega_0/c$. Now we split the annihilation operator into two summands:

$$a(\omega_0 + \Omega) = A_0\delta(0) + a'(\omega_0 + \Omega).$$

For convenience we change notation $a' \rightarrow a$ since we do not need old a any further. Extending now the lower limit of integration to $-\infty$ (since $|\Omega| \ll \omega_0$), we finally obtain the double-sided (from $-\infty$ to $+\infty$) expression for the field operator:

$$\begin{aligned} A(x, t) &= \sqrt{\frac{2\pi\hbar\omega_0}{Sc}} e^{-i(\omega_0 t - k_0 x)} \\ &\times \left[A_0 + \int_{-\infty}^{+\infty} a(\omega_0 + \Omega) e^{-i\Omega(t-x/c)} \frac{d\Omega}{2\pi} \right] \\ &+ \text{h.c.} \end{aligned} \quad (\text{A1})$$

In these notations electric field of the wave is represented as a sum of (i) ‘‘strong’’ (classical) wave with amplitude A_0 and (carrier) frequency ω_0 and (ii) ‘‘weak’’ wave describing the quantum fluctuations of the optical field with its amplitude obeying the commutation relations:

$$\begin{aligned} [a(\omega_0 + \Omega), a(\omega_0 + \Omega')] &= 0, \\ [a(\omega_0 + \Omega), a^\dagger(\omega_0 + \Omega')] &= 2\pi\delta(\Omega - \Omega'). \end{aligned}$$

The double-sided expression is the one most close to the Fourier representation of the classical fields and will be used throughout the paper. For convenience we omit the $\sqrt{2\pi\hbar\omega_0/Sc}$ -multiplier in the main body of the paper since it is the common multiplier in all the equations.

For completeness we also introduce the quadrature components of the wave. Formula (A1) can be rewritten as:

$$A(x, t) = \sqrt{\frac{2\pi\hbar\omega_0}{Sc}} e^{-i(\omega_0 t - k_0 x)}$$

$$\times \left\{ A_0 + \int_0^\infty \left[a_{\omega_0+\Omega} e^{-i\Omega(t-x/c)} + a_{\omega_0-\Omega} e^{i\Omega(t-x/c)} \right] \frac{d\Omega}{2\pi} \right\} + \text{h.c.}, \quad (\text{A2})$$

where $a_{\omega_0-\Omega}$ obeys the same commutation relation as $a_{\omega_0+\Omega}$:

$$[a_{\omega_0+\Omega}, a_{\omega_0+\Omega'}^\dagger] = [a_{\omega_0-\Omega}, a_{\omega_0-\Omega'}^\dagger] = 2\pi\delta(\Omega - \Omega').$$

Next we introduce the so-called correlated two-photon modes with field operators [55, 56]

$$a_c(\Omega) = \frac{a_{\omega_0+\Omega} + a_{\omega_0-\Omega}^\dagger}{\sqrt{2}}, \quad a_s(\Omega) = \frac{a_{\omega_0+\Omega} - a_{\omega_0-\Omega}^\dagger}{\sqrt{2}i},$$

with the only non-zero commutators

$$[a_c, a_{s'}^\dagger] = [a_{c'}, a_s^\dagger] = 2\pi i\delta(\Omega - \Omega'),$$

where prime denotes the argument with Ω' . In terms of these two-photon modes formula (A2) takes the form:

$$A(x, t) = \sqrt{\frac{4\pi\hbar\omega_0}{Sc}} \left[\sqrt{2}A_0 \cos(\omega_0 t - k_0 x) + a_c(x, t) \cos(\omega_0 t - k_0 x) + a_s(x, t) \sin(\omega_0 t - k_0 x) \right], \quad (\text{A3})$$

where operators

$$a_c(x, t) = \int_0^\infty a_c(\Omega) e^{-i\Omega(t-x/c)} \frac{d\Omega}{2\pi} + \text{h.c.}, \quad (\text{A4a})$$

$$a_s(x, t) = \int_0^\infty a_s(\Omega) e^{-i\Omega(t-x/c)} \frac{d\Omega}{2\pi} + \text{h.c.}, \quad (\text{A4b})$$

in the case $A_0 = 0$ are called the cosine and sine quadratures (or quadrature components) correspondingly.

We will also need the double-sided expressions of the quadratures which are obtained from formulas (A4a), (A4b) and conditions $a_{c,s}(\Omega) = a_{c,s}^\dagger(-\Omega)$:

$$a_c(x, t) = \int_{-\infty}^{+\infty} a_c(\Omega) e^{-i\Omega(t-x/c)} \frac{d\Omega}{2\pi},$$

$$a_s(x, t) = \int_{-\infty}^{+\infty} a_s(\Omega) e^{-i\Omega(t-x/c)} \frac{d\Omega}{2\pi}.$$

APPENDIX B: BOUNDARY CONDITIONS

In this Appendix we solve the set of equations (11a – 11d).

First we substitute fields (6 – 10) into this set and separate the 0th and the 1st order sets.

The zeroth order set is:

$$\begin{aligned} A_{+0} &= T A_{\text{in}0} - R A_{-0}, \\ A_{\text{out}0}^r &= R A_{\text{in}0} + T A_{-0}, \\ A_{-0} &= -R A_{+0} e^{2i\omega_1\tau}, \\ A_{\text{out}0}^t &= T A_{+0} e^{i\omega_1\tau}. \end{aligned}$$

Corresponding solution is:

$$\begin{aligned} A_{+0} &= \frac{T}{1 - R^2 e^{2i\omega_1\tau}} A_{\text{in}0}, \\ A_{-0} &= -\frac{RT e^{2i\omega_1\tau}}{1 - R^2 e^{2i\omega_1\tau}} A_{\text{in}0}, \\ A_{\text{out}0}^t &= \frac{T^2 e^{i\omega_1\tau}}{1 - R^2 e^{2i\omega_1\tau}} A_{\text{in}0}, \\ A_{\text{out}0}^r &= \frac{R - R e^{2i\omega_1\tau}}{1 - R^2 e^{2i\omega_1\tau}} A_{\text{in}0}. \end{aligned}$$

Amplitudes $A_{\text{in}0}$, $A_{\pm 0}$ and $A_{\text{out}0}^r$ are evaluated at point $x = 0$ and amplitude $A_{\text{out}0}^t$ at point $x = L$.

The first order solution in spectral domain is:

$$\begin{aligned} a_+ &= T a_{\text{in}} - R a_- + R A_{-0} 2ik_1 X_a, \\ a_{\text{out}}^r &= R a_{\text{in}} + T a_- + R A_{\text{in}0} 2ik_1 X_a, \\ a_- &= T a_{\text{vac}} e^{i(\omega_1+\Omega)\tau} - R a_+ e^{2i(\omega_1+\Omega)\tau} \\ &\quad - R A_{+0} e^{2i\omega_1\tau} \left[2ik_1 X_b + g_+(L) - g_-(L) \right. \\ &\quad \left. + w_+(L) - w_-(L) \right] e^{i\Omega\tau}, \\ a_{\text{out}}^t &= R a_{\text{vac}} + T a_+ e^{i(\omega_1+\Omega)\tau}. \end{aligned}$$

Here $a_i = a_i(\omega_1 + \Omega)$, $g_\pm(x) = g_\pm(x, \omega_1 + \Omega)$ and $X_i = X_i(\Omega)$. Spectral amplitudes a_{in} , a_\pm and a_{out}^r are evaluated at point $x = 0$ and amplitude a_{out}^t at point $x = L$. The first order solution is:

$$\begin{aligned} a_+ &= \frac{T}{1 - R^2 e^{2i(\omega_1+\Omega)\tau}} a_{\text{in}} - \frac{RT e^{i(\omega_1+\Omega)\tau}}{1 - R^2 e^{2i(\omega_1+\Omega)\tau}} a_{\text{vac}} + \frac{R^2 A_{+0} e^{2i\omega_1\tau}}{1 - R^2 e^{2i(\omega_1+\Omega)\tau}} i \left[2k_1 (X_b e^{i\Omega\tau} - X_a) + \delta\Psi_{\text{emw}} \right], \\ a_- &= -\frac{RT e^{2i(\omega_1+\Omega)\tau}}{1 - R^2 e^{2i(\omega_1+\Omega)\tau}} a_{\text{in}} + \frac{T e^{i(\omega_1+\Omega)\tau}}{1 - R^2 e^{2i(\omega_1+\Omega)\tau}} a_{\text{vac}} + \frac{A_{-0}}{1 - R^2 e^{2i(\omega_1+\Omega)\tau}} i \left[2k_1 (X_b e^{i\Omega\tau} - \rho_1 X_a) + \delta\Psi_{\text{emw}} \right], \\ a_{\text{out}}^t &= \frac{T^2 e^{i(\omega_1+\Omega)\tau}}{1 - R^2 e^{2i(\omega_1+\Omega)\tau}} a_{\text{in}} + \frac{R - R e^{2i(\omega_1+\Omega)\tau}}{1 - R^2 e^{2i(\omega_1+\Omega)\tau}} a_{\text{vac}} + \frac{R^2 A_{\text{out}0}^t e^{2i\omega_1\tau}}{1 - R^2 e^{2i(\omega_1+\Omega)\tau}} i \left[2k_1 (X_b e^{i\Omega\tau} - X_a) + \delta\Psi_{\text{emw}} \right] e^{i\Omega\tau}, \end{aligned}$$

$$a_{\text{out}}^r = \frac{R - Re^{2i(\omega_1+\Omega)\tau}}{1 - R^2e^{2i(\omega_1+\Omega)\tau}} a_{\text{in}} + \frac{T^2e^{i(\omega_1+\Omega)\tau}}{1 - R^2e^{2i(\omega_1+\Omega)\tau}} a_{\text{vac}} + \frac{TA_{-0}}{1 - R^2e^{2i(\omega_1+\Omega)\tau}} i \left[2k_1 \left(X_b e^{i\Omega\tau} - \sigma_1 X_a \right) + \delta\Psi_{\text{emw}} \right],$$

where $\rho_1(\Omega) = R^2e^{2i(\omega_1+\Omega)\tau}$. Phase shift $\delta\Psi_{\text{emw}}$ and factor σ_1 are introduced in Sec. III.

-
- [1] R. Weiss, Quarterly Progress Report, Research Lab. of Electronics, M.I.T. **105**, 54 (1972).
- [2] L. Ju, D.G. Blair and C. Zhao, Rep. Prog. Phys. **63**, 1317 (2000).
- [3] A. Abramovici *et al.*, Science **256**, 325 (1992).
- [4] D. Sigg *et al.*, Class. Quantum Grav. **23**, S51 (2006).
- [5] *LIGO website*, URL <http://www.ligo.caltech.edu>.
- [6] F. Acernese *et al.*, Class. Quantum Grav. **23**, S635 (2006).
- [7] *VIRGO website*, URL <http://www.virgo.infn.it>.
- [8] H. Luck *et al.*, Class. Quantum Grav. **23**, S71 (2006).
- [9] *GEO-600 website*, URL <http://geo600.aei.mpg.de>.
- [10] M. Ando *et al.*, Class. Quantum Grav. **22**, S881 (2005).
- [11] *TAMA-300 website*, URL <http://tamago.mtk.nao.ac.jp>.
- [12] D.E. McClelland *et al.*, Class. Quantum Grav. **23**, S41 (2006).
- [13] *ACIGA website*, URL <http://www.anu.edu.au/Physics/ACIGA>.
- [14] A. Weinstein, Class. Quantum Grav. **19**, 1575 (2002).
- [15] *Advanced LIGO website*, URL <http://www.ligo.caltech.edu/advLIGO/scripts/summary>.
- [16] K. Kuroda, Class. Quantum Grav. **23**, S215 (2006).
- [17] V.B. Braginsky and F.Ya. Khalili, *Quantum Measurement* (Cambridge University Press, Cambridge, 1992).
- [18] V.B. Braginsky, Sov. Phys. JETP **26**, 831 (1968).
- [19] V.B. Braginsky and Yu.I. Vorontsov, Sov. Phys. Usp. **17**, 644 (1975).
- [20] V.B. Braginsky, Yu.I. Vorontsov and F.Ya. Khalili, Sov. Phys. JETP **46**, 705 (1977).
- [21] H.J. Kimble *et al.*, Phys. Rev. D **65**, 022002 (2002), arXiv:gr-qc/0008026v2.
- [22] F.Ya. Khalili, Phys. Lett. A **298**, 308 (2002), arXiv:gr-qc/0203002v1.
- [23] S.L. Danilishin and F.Ya. Khalili, Phys. Lett. A **300**, 547 (2002), arXiv:gr-qc/0202100v4.
- [24] F.Ya. Khalili, Phys. Lett. A **317**, 169 (2003), arXiv:gr-qc/0304060v1.
- [25] S.L. Danilishin and F.Ya. Khalili, Phys. Rev. D **73**, 022002 (2006), arXiv:gr-qc/0508022v1.
- [26] F.Ya. Khalili, Phys. Rev. D **75**, 082003 (2007).
- [27] S. Kawamura and Y. Chen, Phys. Rev. Lett. **93**, 211103 (2004), arXiv:gr-qc/0405093v2.
- [28] Y. Chen and S. Kawamura, Phys. Rev. Lett. **96**, 231102 (2006), arXiv:gr-qc/0504108v3.
- [29] Y. Chen *et al.*, Phys. Rev. Lett. **97**, 151103 (2006), arXiv:gr-qc/0603054v2.
- [30] C.M. Caves, Phys. Rev. D **23**, 1693 (1981), arXiv:gr-qc/0405093v2.
- [31] W.K. Unruh, *Experimental Gravitation, and Measurement Theory* (Plenum, New York, 1982), p. 647.
- [32] V.B. Braginsky and F.Ya. Khalili, Rev. Mod. Phys. **68**, 1 (1996).
- [33] C. Misner, K. Thorne and J. Wheeler, *Gravitation*, vol. 3 (San Francisco, W.H. Freeman and Company, 1973).
- [34] E.E. Flanagan and S.A. Hughes, New J. Phys. **7**, 204 (2005), arXiv:gr-qc/0501041v3.
- [35] R. Blandford and K.S. Thorne, *Ph 136: Applications of Classical Physics* (California Institute of Technology, Pasadena, 2003), chap. 26, URL <http://www.pma.caltech.edu/Courses/ph136/yr2002/chap26/0223>.
- [36] M. Rakhmanov, Phys. Rev. D **71**, 084003 (2005), arXiv:gr-qc/0406009v1.
- [37] S.P. Tarabrin, Phys. Rev. D **75**, 102002 (2007), arXiv:gr-qc/0701156v2.
- [38] K. Somiya *et al.*, Phys. Rev. Lett. **76**, 022002 (2007).
- [39] S.P. Vyatchanin, paper in preparation.
- [40] V.B. Braginsky and A.B. Manukin, Sov. Phys. JETP **25**, 653 (1967).
- [41] V.B. Braginsky, M.L. Gorodetsky and F.Ya. Khalili, Phys. Lett. A **232**, 340 (1997).
- [42] V.B. Braginsky and F.Ya. Khalili, Phys. Lett. A **257**, 241 (1999).
- [43] M. Rakhmanov, Ph.D. thesis, California Institute of Technology (2000), URL <http://www.ligo.caltech.edu/docs/P/P000002-00.pdf>.
- [44] F.Ya. Khalili, Phys. Lett. A **288**, 251 (2001), arXiv:gr-qc/0107084.
- [45] A. Buonanno and Y. Chen, Phys. Rev. D **64**, 042006 (2001), arXiv:gr-qc/0102012.
- [46] A. Buonanno and Y. Chen, Phys. Rev. D **65**, 042001 (2001), arXiv:gr-qc/0107021.
- [47] V.I. Lazebny and S.P. Vyatchanin, Phys. Lett. A **344**, 7 (2005).
- [48] F.Ya. Khalili, V.I. Lazebny and S.P. Vyatchanin, Phys. Rev. D **73**, 062002 (2006), arXiv:gr-qc/0511008.
- [49] S.P. Tarabrin, paper in preparation.
- [50] W.-T. Ni and M. Zimmermann, Phys. Rev. D **17**, 1473 (1978).
- [51] K.-P. Marzlin, Phys. Rev. D **50**, 888 (1994).
- [52] R. Blandford and K.S. Thorne, *Ph 136: Applications of Classical Physics* (California Institute of Technology, Pasadena, 2003), chap. 23, URL <http://www.pma.caltech.edu/Courses/ph136/yr2002/chap26/0223>.
- [53] C.K. Law, Phys. Rev. A **51**, 2537 (1995).
- [54] S.P. Tarabrin and S.P. Vyatchanin, paper in preparation.
- [55] C.M. Caves and B.L. Schumaker, Phys. Rev. A **31**, 3068 (1985).
- [56] B.L. Schumaker and C.M. Caves, Phys. Rev. A **31**, 3093 (1985).